

Nitrogen-Activated Transitions, Level Repulsion, and Band Gap Reduction in GaAs_{1-x}N_x with $x < 0.03$

J. D. Perkins, A. Mascarenhas, Yong Zhang, J. F. Geisz, D. J. Friedman, J. M. Olson, and Sarah R. Kurtz

National Renewable Energy Laboratory, Golden, Colorado 80401-3393

(Received 12 November 1998)

We report electroreflectance spectra for a series of GaAs_{1-x}N_x samples with $x < 0.03$. For all samples, the fundamental band gap transition (E_0) and the transition from the spin-orbit split-off valence band ($E_0 + \Delta_0$) are observed. For samples with $x \geq 0.008$, an additional transition (E_+) is observed. With increasing nitrogen content, the increase in E_+ is linear in, and nearly equal to, the band gap reduction indicative of a nitrogen-induced level repulsion. The directly observed E_+ transition may arise from either a nitrogen-related resonant level or a disorder-activated indirect transition. [S0031-9007(99)08950-4]

PACS numbers: 71.20.Nr, 71.55.Eq, 78.20.-e, 78.66.Fd

Substituting just one percent nitrogen for arsenic in GaAs decreases the room temperature band gap from 1.42 to 1.25 eV [1,2]. This is quite remarkable considering that GaN has a band gap nearly 2 eV higher, not lower, than that of GaAs. In contrast, for conventional III-V alloys, such as Ga_{1-x}In_xAs, the deviation of the band gap energy from that of a composition weighted linear average is usually small and well described by the quadratic correction $\Delta E_g(x) = bx(x - 1)$ with b of order 0.5 eV [3]. To parametrize the measured band gap reduction of GaAs_{1-x}N_x in this way requires introducing a composition dependent bowing coefficient, $b(x)$, of order 10–20 eV [4–6]. This incongruity suggests that, for GaAsN, the origins of the band gap energy's composition dependence differ from those for conventional III-V alloys [3]. Hence, understanding the band gap reduction in the particular material GaAsN will likely improve the understanding of semiconductor alloys in general. However, other than the ubiquitously observed decrease in the band gap energy with increasing nitrogen content [4,5,7–9], there has been little experimental evidence regarding the cause of the large band gap reduction in GaAs_{1-x}N_x until very recently [10]. Furthermore, it is precisely this band gap reduction which makes GaAsN and GaInAsN alloys of technological interest for integrated light emitting electronics, infrared diode lasers [11], and multijunction high efficiency solar cells [12].

In this Letter, we present room-temperature electroreflectance spectra for a series of GaAs_{1-x}N_x samples with $x < 0.03$ as well as two quaternary samples with compositions Ga_{0.95}In_{0.05}As_{0.987}N_{0.013} and Ga_{0.92}In_{0.08}As_{0.978}N_{0.022}. For all ten samples, we observe both the fundamental band gap transition (E_0) as well as the transition from the spin-orbit split-off valence band ($E_0 + \Delta_0$). An additional transition (denoted E_+) is observed for the GaAs_{1-x}N_x samples with $x \geq 0.008$. Unlike E_0 and $E_0 + \Delta_0$, which decrease in energy with increasing nitrogen content, E_+ increases with increasing nitrogen content. A mutual repulsion between the E_+ level and

the conduction band minimum, as manifest by the directly observed divergence of E_0 and E_+ , would account for the unusually large band gap reduction in nitrogen substituted GaAs. The E_+ transition may arise from either a nitrogen-related resonant level within the conduction band or from a disorder-activated indirect transition such as $\Gamma_v \rightarrow L_c$.

Epitaxial GaAsN and GaInAsN samples were grown on Zn doped (001) GaAs substrates by atmospheric-pressure metallic-organic vapor phase epitaxy (MOVPE) using trimethylgallium, arsine, trimethylindium, and dimethylhydrazine (nitrogen) sources [12]. Sample temperatures during growth ranged from 570 to 650 °C. The nitrogen content was determined from either, or both, x-ray diffraction and secondary ion mass spectroscopy. The sample thickness ranged from 1 to 7 μm .

Room-temperature electroreflectance spectra were measured using a contactless electroreflectance technique [13]. The spectra were measured in a near normal incidence geometry using a scanning monochromator with a broad band tungsten-filament bulb as a light source. The unmodulated probe beam was focused to a roughly 1 mm \times 4 mm spot on the sample. The reflected light was refocused into either a Si or LN₂ cooled InGaAs photodiode detector as appropriate for the wavelength being measured. A lock-in amplifier was used to measure the change in reflectance due to a modulating voltage of ± 750 to 1000 V at 400 Hz.

Figure 1 shows the electroreflectance spectra for a 2 μm thick GaAs_{0.978}N_{0.022} sample. For the modulation voltages used, roughly ± 1000 V across 1 mm, the corresponding field, 10 KV/cm, yields electroreflectance spectra in the low-field regime where the measured $\Delta R/R$ spectra correspond to the third energy derivative of the dielectric function [14]. Hence, sharp derivativelike features are expected at energies corresponding to critical points in the electronic structure. In Fig. 1, three such features, labeled E_0 , $E_0 + \Delta_0$, and E_+ , are seen at photon energies of 1.19, 1.52, and 1.83 eV, respectively. The latter two features, $E_0 + \Delta_0$ and E_+ , are more clearly seen in the second spectra shown which is displayed with

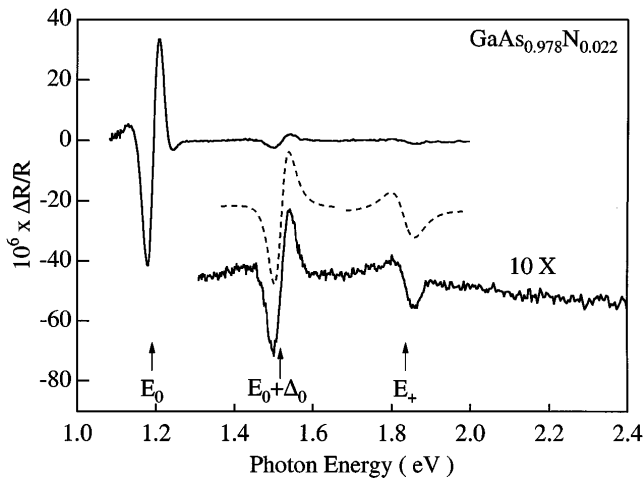


FIG. 1. Electroreflectance spectra for a $2 \mu\text{m}$ thick $\text{GaAs}_{0.978}\text{N}_{0.022}$ film on a GaAs substrate. The band gap transition (E_0) at 1.19 eV as well as the transition from the spin-orbit split-off valence band ($E_0 + \Delta_0$) at 1.52 eV are easily seen. An additional weak feature (E_+) at 1.83 eV is more clearly seen in the second spectra shown at 10 \times and offset for clarity. The fitted line shape for the $E_0 + \Delta_0$ and E_+ transitions are shown with dashed lines and offset for clarity.

a factor of 10 magnification and offset vertically. The strong E_0 transition at 1.19 eV with $\Delta R/R \approx 4 \times 10^{-5}$ corresponds to the direct band gap excitation at $k = 0$. The weaker, but still easily observed, $E_0 + \Delta_0$ transition at 1.52 eV with $\Delta R/R = 3 \times 10^{-6}$ corresponds to the transition from the spin-orbit split-off valence band to the conduction band minimum at $k = 0$. The measured spin-orbit valence band splitting of ~ 0.33 eV is close to that of bulk GaAs and to the 0.33 eV we measure for a pure GaAs film. The transition energies, indicated by vertical arrows in Fig. 1, are determined by fitting the measured spectra to the Aspnes third-derivative functional form $\Delta R/R = \text{Re}\{C e^{i\theta} / (E - E_i + i\Gamma)^{5/2}\}$ [14]. The resultant fits for the $E_0 + \Delta_0$ and E_+ transitions are shown in Fig. 1 with dashed lines and offset for clarity.

In addition to the E_0 and $E_0 + \Delta_0$ transitions which are intrinsic to zinc blende III-V semiconductors, a third weaker feature, denoted E_+ , with $\Delta R/R \approx 1 \times 10^{-6}$ is observed at higher energy, 1.83 eV. This E_+ transition is observed only in $\text{GaAs}_{1-x}\text{N}_x$ samples with $x \geq 0.008$. Neither the spin-orbit $E_0 + \Delta_0$ nor the E_+ transition were observed in recent contactless electroreflectance measurements [9]. This is likely due to the masking of these weak transitions by the strong features from the GaAs substrate which are observable for the partially transparent 4000 Å thick GaAsN layers examined in Ref. [9]. In our measurements, the optically thick ($2 \mu\text{m}$) GaAsN layer suppresses any possible substrate related features, thereby enabling our observation of the $E_0 + \Delta_0$ and E_+ features.

Figure 2 shows electroreflectance spectra for eight GaAsN samples [Figs. 2(a)–2(h)] and two GaInAsN samples [Figs. 2(i) and 2(j)]. Note the different scales

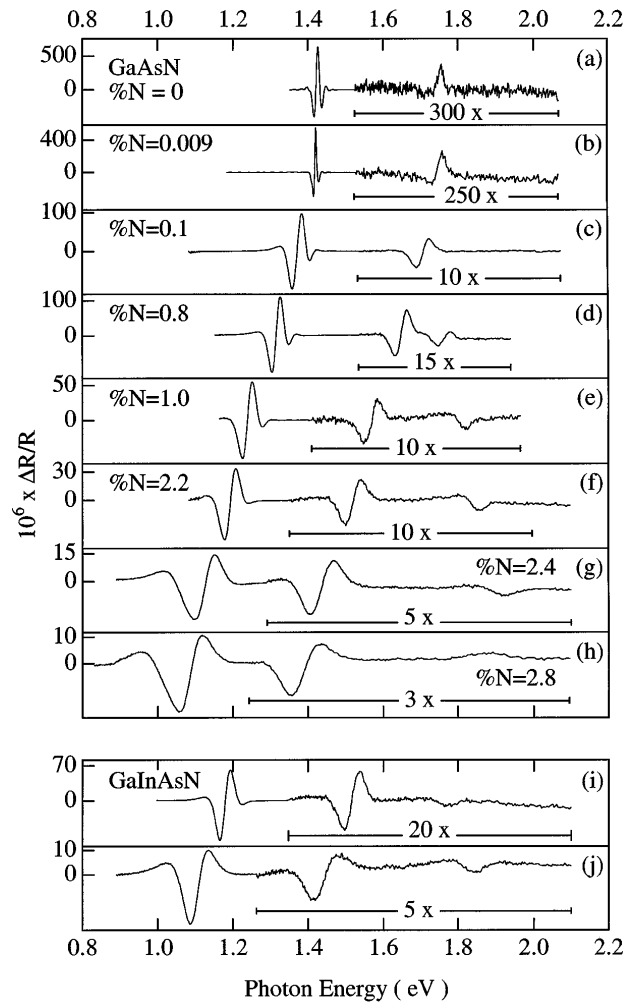


FIG. 2. Electroreflectance spectra for $\text{GaAs}_{1-x}\text{N}_x$ [(a)–(h)] and GaInAsN [(i) and (j)]. Note the different scale used for each panel as well as the expanded scale within each panel used to more clearly display the above band gap transitions. For the $\text{GaAs}_{1-x}\text{N}_x$ samples, the nitrogen content ranges from $x = 0$ (a) to $x = 0.028$ (h). For the GaInAsN samples, the compositions are $\text{Ga}_{0.95}\text{In}_{0.05}\text{As}_{0.987}\text{N}_{0.013}$ (i) and $\text{Ga}_{0.92}\text{In}_{0.08}\text{As}_{0.978}\text{N}_{0.022}$ (j).

used for each panel as well as the expanded scale used within each panel to more clearly display the above band gap transitions. For the $\text{GaAs}_{1-x}\text{N}_x$ spectra, the nitrogen content of the samples increases monotonically from $x = 0$ [Fig. 2(a)] to $x = 0.028$ [Fig. 2(h)]. The relative uncertainty in nitrogen content is estimated to be $\pm 20\%$. The well-established decrease in the band gap energy with increasing nitrogen content is clear. In addition, the spin-orbit split-off $E_0 + \Delta_0$ transition is observed for each sample and tracks the energy shift of the band gap with a nearly constant splitting of ~ 0.3 eV. We also note the general decrease in strength and increase in width of the E_0 band gap feature with increasing nitrogen content.

In addition to the E_0 and $E_0 + \Delta_0$ transitions observed in all of the samples, the extra E_+ transition is apparent for the $\text{GaAs}_{1-x}\text{N}_x$ samples with $x \geq 0.008$

[Figs. 2(d)–2(h)]. In contrast to E_0 and $E_0 + \Delta_0$, which decrease in energy with increasing nitrogen content, E_+ generally increases in energy with increasing nitrogen content. The only exception being the highest nitrogen content sample shown in Fig. 2(h) where the E_+ transition is slightly lower in energy than that for the sample in Fig. 2(g). However, unlike the samples with $x \leq 0.024$ which have a mirrorlike surface, the sample of Fig. 2(h) has a noticeably lined surface indicative of structural defects due to the large lattice mismatch, $\sim 0.6\%$. Still, the observation of the E_+ transition in this sample supports the generality of the E_+ transition. Finally, in the bottom two panels, we show electroreflectance spectra for two quaternary alloys with compositions $\text{Ga}_{0.95}\text{In}_{0.05}\text{As}_{0.987}\text{N}_{0.013}$ [Fig. 2(i)] and $\text{Ga}_{0.92}\text{In}_{0.08}\text{As}_{0.978}\text{N}_{0.022}$ [Fig. 2(j)] which are lattice matched to GaAs. All three of the electroreflectance features seen in Fig. 1 can be seen in each of the two quaternary alloy samples. This demonstrates that the observation of the E_+ transition is not dependent upon the strain intrinsic to the GaAsN samples and further supports the generality of the E_+ transition.

The decrease of $E_0 + \Delta_0$ and the increase in E_+ with increasing nitrogen content are both evident in Fig. 2. However, as shown in Fig. 3, the systematic trends are clearer when the energy differences, $E_+ - E_0$ (\bullet) and Δ_0 (\blacktriangle), are plotted versus the band gap reduction, $\delta E_0 = E_0(0) - E_0(x)$. The solid symbols are for the GaAsN samples and the open symbols for the GaInAsN samples. When plotted in this way, the composition independence of Δ_0 and the linear increase in $E_+ - E_0$ for $\delta E_0 < 0.3$ eV are clear. Since the energy splittings $E_+ - E_0$ and Δ_0 are comparable, their different composition dependencies (i.e., the composition independence of Δ_0) show that the E_+ transition does not correspond to an electronic transition from within the valence band to the conduction band minimum. Hence, we conclude that the E_+ transition corresponds to an electronic transition between the valence band maximum and a level above the conduction band minimum.

For the first four $\text{GaAs}_{1-x}\text{N}_x$ samples for which the E_+ transition is observed ($0.008 < x < 0.024$), the increase

in $E_+ - E_0$ is linear. The dashed line in Fig. 3, a linear fit to these four $E_+ - E_0$ points, has a slope of 1.67. Linear extrapolation to the dilute limit, $\delta E_0 = 0$, of the E_+ transition in $\text{GaAs}_{1-x}\text{N}_x$ yields $E_+ - E_0(x = 0^+) = 0.26$ eV or $E_+(x = 0^+) = 1.68$ eV. However, no E_+ transition is observed in the electroreflectance spectra for samples with $x \leq 0.001$. Taking into account the factor of δE_0 implicit in $E_+ - E_0$ and defining $\delta E_+ = E_+(x) - E_+(x = 0^+)$, yields $\delta E_+ = 0.67\delta E_0$.

The opposite and nearly equal shifts of E_+ and E_0 with increasing nitrogen content suggest that a nitrogen-induced level repulsion contributes to the observed band gap reduction. For the two quaternary GaInAsN samples shown with open symbols in Fig. 3, $E_+ - E_0$ and Δ_0 show the same trends as observed in the ternary GaAsN samples. However, while Δ_0 in the quaternary is essentially the same as that in the ternary, $E_+ - E_0$ is smaller than that observed for a ternary sample with the same band gap reduction δE_0 . This is consistent with a nitrogen-induced level repulsion between E_+ and E_0 contributing to the band gap reduction since in the quaternary alloy some of the band gap reduction is due to In substitution. We next consider what electronic states might interact with the conduction band minimum to produce the observed interaction between E_+ and E_0 .

Nitrogen substitution into GaAs destroys the formal translational symmetry underlying momentum conservation based optical selection rules and thereby may make normally forbidden indirect transitions optically active. In particular, our extrapolated value for $E_+(x = 0^+) = 1.68$ eV is close to the 1.71 eV room-temperature $\Gamma_v \rightarrow L_c$ energy difference in GaAs [15]. First principles calculations find that the direct E_0 optical transition is strongly suppressed in dilutely nitrogen substituted GaAs [16]. By conservation of oscillator strength, indirect transitions such as $\Gamma_v \rightarrow L_c$ could become observable. Further calculations find that N substitution for As induces intraband coupling within both the conduction and valence bands [6]. Such intraband coupling causes intraband level repulsion which, in addition to decreasing the conduction band minimum, could increase the L -point energy, consistent with the observed divergence of the E_0 and E_+ levels. Additional, very recent, calculations do find that the L -point energy increases with nitrogen substitution [17].

Alternatively, very recent pressure-dependent photomodulation measurements observe a saturation in the increase of the apparent band gap energy with increasing hydrostatic pressure in GaInAsN containing small amounts of nitrogen, a few percent or less [10]. This is explained using a simple two level anticrossing model including a normally pressure-dependent GaAs-like band gap and a nominally pressure-independent nitrogen level. This simple model provides a good fit to the measured data with E_N , the nitrogenlike level, ~ 1.74 eV above the valence band maximum. Photoluminescence from nitrogen trapped excitons has been observed in both nitrogen doped GaAs:N under hydrostatic pressure [18,19] and nitrogen

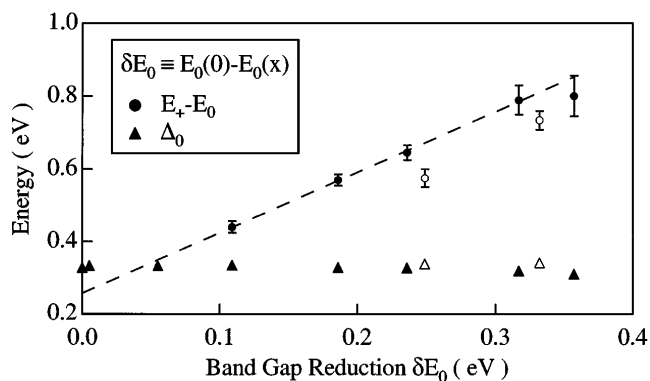


FIG. 3. Energy differences vs the band gap reduction: the spin-orbit splitting Δ_0 (\blacktriangle) and $E_+ - E_0$ (\bullet). Solid symbols are for GaAsN and open symbols for GaInAsN.

doped $\text{GaAs}_{1-x}\text{P}_x\text{:N}$ for $x \geq 0.2$ [20]. Extrapolation of the nitrogen bound exciton energy back either to ambient pressure for GaAs:N or to GaAs:N for $\text{GaAs}_{1-x}\text{P}_x\text{:N}$ yields energies of 1.65 and 1.7 eV, respectively, close to our extrapolated value of 1.68 eV. Hence, considering energies alone, a nitrogenlike E_+ level at $E_+ \approx 1.7$ eV is reasonable. Furthermore, in GaAs:N at hydrostatic pressure slightly lower than that necessary for the nitrogen bound exciton to become nonresonant, LO phonon sidebands were observed indicating that the nitrogen level remains spatially localized even when resonant within the conduction band [18]. Such a spatially localized level includes momentum components from across the entire Brillouin zone, thus enabling pseudodirect optical transitions.

In summary, we have presented room-temperature electroreflectance spectra for a series of $\text{GaAs}_{1-x}\text{N}_x$ samples with $x < 0.03$ as well as two quaternary alloys with compositions $\text{Ga}_{0.95}\text{In}_{0.05}\text{As}_{0.987}\text{N}_{0.013}$ and $\text{Ga}_{0.92}\text{In}_{0.08}\text{As}_{0.978}\text{N}_{0.022}$. For all samples, both the fundamental band gap transition (E_0) as well as the transition from the spin-orbit split-off valence band ($E_0 + \Delta_0$) are observed. For the GaAsN samples, the band gap energy decreases monotonically with increasing nitrogen content and the spin-orbit split-off transition shifts with the band gap at constant offset of ~ 0.3 eV. In addition, for the $\text{GaAs}_{1-x}\text{N}_x$ samples with $x \geq 0.008$, an additional transition (E_+) is observed. Unlike the band gap and spin-orbit transitions, E_+ increases in energy with increasing nitrogen content. The lack of interaction between $E_0 + \Delta_0$ and E_+ indicates that the E_+ transition corresponds to an electronic transition between the valence band maximum and a level above the conduction band minimum. The observed E_+ transition may arise from either a nitrogen-related resonant level ~ 0.25 eV above the conduction band minimum in the dilute limit or from a disorder-activated indirect transition such as $\Gamma_v \rightarrow L_c$. However, independent of the exact nature of the E_+ transition, the opposite and nearly equal shifts of E_0 and E_+ we directly observe show that a nitrogen-induced level repulsion contributes to the unusually large band gap reduction in nitrogen substituted GaAs.

We thank W. Walukiewicz for informative discussions regarding their pressure-dependent photomodulation mea-

surements prior to publication. We also thank C. Kramer for help with sample preparation and B. Reedy for SIMS measurements along with H. Cheong and A. Zunger for informative discussions. This work was supported by the Office of Energy Efficiency of the Department of Energy under Contract No. DE-AC36-83CH10093.

-
- [1] M. Weyers, M. Sato, and H. Ando, *Jpn. J. Appl. Phys.* **31**, L853 (1992).
 - [2] J. Salzman and H. Temkin, *Mater. Sci. Eng. B* **50**, 148 (1997).
 - [3] A.-B. Chen and A. Sher, *Semiconductor Alloys Physics and Materials Engineering* (Plenum, New York, 1995).
 - [4] W. G. Bi and C. W. Tu, *Appl. Phys. Lett.* **70**, 1608 (1997).
 - [5] K. Uesugi and I. Suemune, *Jpn. J. Appl. Phys.* **36**, L1572 (1997).
 - [6] S.-H. Wei and A. Zunger, *Phys. Rev. Lett.* **76**, 664 (1996).
 - [7] S. Francoeur, G. Sivaraman, Y. Qiu, S. Nikishin, and H. Temkin, *Appl. Phys. Lett.* **72**, 1857 (1998).
 - [8] T. Makimoto, H. Saito, T. Nishida, and N. Kobayashi, *Appl. Phys. Lett.* **70**, 2984 (1997).
 - [9] L. Malikova, F. H. Pollak, and R. Bhat, *J. Electron. Mater.* **27**, 484 (1998).
 - [10] W. Shan *et al.*, *Phys. Rev. Lett.* **82**, 1221 (1999).
 - [11] M. Kondow, S. Nakatsuka, T. Kitatani, Y. Yazawa, and M. Okai, *Jpn. J. Appl. Phys.* **35**, 5711 (1996).
 - [12] J. F. Geisz, D. J. Friedman, J. M. Olson, S. R. Kurtz, and B. M. Keyes, *J. Cryst. Growth* **195**, 401 (1998).
 - [13] X. Yin and F. H. Pollak, *Appl. Phys. Lett.* **59**, 2305 (1991).
 - [14] D. E. Aspnes, *Surf. Sci.* **37**, 418 (1973).
 - [15] J. S. Blakemore, *J. Appl. Phys.* **53**, R123 (1982).
 - [16] L. Bellaiche, S.-H. Wei, and A. Zunger, *Phys. Rev. B* **56**, 10 233 (1997).
 - [17] E. D. Jones *et al.* (unpublished).
 - [18] D. J. Wolford, J. A. Bradley, K. Fry, and J. Thompson, in *Proceedings of the 17th International Conference on the Physics of Semiconductors*, edited by J. D. Chadi and W. A. Harrison (Springer, New York, 1985).
 - [19] X. Liu, M.-E. Pistol, L. Samuelson, S. Schwetlick, and W. Seifert, *Appl. Phys. Lett.* **56**, 1451 (1990).
 - [20] D. J. Wolford, W. Y. Hsu, J. D. Dow, and B. G. Streetman, *J. Lumin.* **18/19**, 863 (1979).